Original article

Novel methods to diagnose rotator cuff tear and predict post-operative Re-tear: Radiomics models

Yang Fei [a,b,c,1], Yidong Wan [d,e,1], Lei Xu [g,1], Zizhan Huang [a,b,c], Dengfeng Ruan [a,b,c], Canlong Wang [a,b,c], Peiwen He [a,b,c], Xiaozhong Zhou [a,b,c], Boon Chin Heng [f], Tianye Niu [d,e,**], Weiliang Shen [a,b,c,***], Yan Wu [a,b,c,*]

[a] Department of Orthopedics, The Second Affiliated Hospital, Zhejiang University School of Medicine, Hangzhou, Zhejiang, China
[b] Key Laboratory of Motor System Disease Research and Precision Therapy of Zhejiang Province, Hangzhou, Zhejiang, China
[c] Orthopedics Research Institute of Zhejiang University, Hangzhou, Zhejiang, China
[d] Sir Run Run Shaw Hospital, Zhejiang University School of Medicine, Hangzhou, Zhejiang, China
[e] Institute of Translational Medicine, Zhejiang University, Hangzhou, Zhejiang, China
[f] School of Stomatology, Peking University, Beijing, China
[g] Department of Radiation Oncology, the First Affiliated Hospital of Xi'an Jiaotong University, Xi'an, Shaanxi, China

ARTICLE INFO

ABSTRACT

Objective: To validated a classifier to distinguish the status of rotator cuff tear and predict post-operative re-tear by utilizing magnetic resonance imaging (MRI) markers.

Methods: This retrospective study included patients with healthy rotator cuff and patients diagnosed as rotator cuff tear (RCT) by MRI. Radiomics features were identified from the pre-operative shoulder MRI and selected by using maximum relevance minimum redundancy (MRMR) methods. A radiomics model for diagnosis of RCT was constructed, based on the 3D volume of interest (VOI) of supraspinatus. Another model for the prediction of rotator re-tear after rotator cuff repair (Re-RCT) was constructed based on VOI of humerus, supraspinatus, infraspinatus and other clinical parameters.

Results: The model for diagnosing the status of RCT produced an area under the receiver operating characteristic curve (AUC) of 0.989 in the training cohort and 0.979 for the validation cohort. The radiomics model for predicting Re-RCT produced an AUC of 0.923 ± 0.017 for the training dataset and 0.790 ± 0.082 for the validation dataset. The nomogram combining radiomics features and clinical factors yielded an AUC of 0.961 ± 0.020 for the training dataset and 0.808 ± 0.081 for the validation dataset, which displayed the best performance among all models.

Conclusion: Radiomics models for the diagnosis of rotator cuff tear and prediction of post-operative Re-RCT yielded a decent prediction accuracy.

1. Background

Rotator cuff tear (RCT) is a common cause of shoulder dysfunction and pain, with rising incidence rate with age. Typically, about 50% of people over the age of 80 have suffered from rotator cuff tears.[1] Various therapeutic modalities have been used for the treatment of rotator cuff injury, with open repair surgical techniques being considered the gold standard in the past. Arthroscopic rotator cuff repair (ARCR), which involve minimal surgical incisions but yield comparable therapeutic effects with open surgery, has now become a standard operation procedure.[2,3]

The complications of ARCR, though, should not to be neglected. The incidence of rotator cuff re-tear (Re-RCT), is one of the most common complications, ranging from 4.5% to 94%,[4,5] which mostly occur during the early post-operative period, especially within 3 months post-surgery.[6] Numerous patient factors result in failure.[7–11] The experience of the surgical team and rehabilitation optimization also influence the

Abbreviations

MRI	Magnetic resonance imaging
RCT	Rotator cuff tear
MRMR	Maximum relevance minimum redundancy
VOI	Volume of interest
Re-RCT	Rotator re-tear after rotator cuff repair
AUC	Area under the receiver operating characteristic curve
ARCR	Arthroscopic rotator cuff repair
MLR	Multiple regression logistic
SVM	Support vector machine
RF	Random forest
ROC	Receiver operating characteristic curve
CI	confidence interval
AIC	Akaike Information Criterion

occurrence of post-operative re-tear.[12,13] However, quantitative criteria for post-operative assessment are still lacking.

Magnetic resonance imaging (MRI) is an essential non-invasive tool in diagnosis and treatment evaluation of rotator cuff injuries.[14] The sensitivity and specificity rates of MRI in the diagnosis of rotator cuff injury are 98% and 79%.[15–17] Sugaya classification based on post-operative MRI, showed favorable correlation with clinical outcomes,[18] and is commonly applied for assessment of the post-operative status of RCT.[19] For the prediction of Re-RCT, experienced surgeons can also make a preliminary judgment on whether the patient is prone to re-tear from MRI. The size of the tear did not influence whether a re-tear would occur, but a common concept is that the larger the tear of the supraspinatus, the more difficult it is to repair.[20] Besides, the reparability is associated with Goutallier classification of the supraspinatus and infraspinatus muscles and the Patte classification.[15] Although radiologists are able to assess the probability of rotator cuff tear and post-operative re-tear using semantic or morphological MRI imaging features together with medical history in clinical practice, this method is still limited by subjectivity and imposed a heavy workload burden.

Recently, radiomics have been widely used to improve the response prediction of clinical tasks via a non-invasive approach. Medical imaging of tumors have extensively been applied in predicting the status of prognosis, grade of pathology and survival prediction, despite the heterogeneity of tumors. Previous studies have developed classifiers to discriminate multiple types of orthopedic diseases.[21,22] These classifiers achieved promising predictive accuracies. However, the radiomics analysis in the domain of rotator cuff injury and prediction of

post-operative re-tear for better clinical management, have not yet been thoroughly investigated.

In this study, we aimed to generate and validate a classifier to distinguish the status of RCT by radiomics features derived from the supraspinatus region. We also evaluated the performance of the radiomics model for predicting re-tear. The re-tear model was also developed, based on radiomics features of the three regions involved: supraspinatus, infraspinatus and humerus.

2. Methods

2.1. Patients

The workflow of analyses carried out in this study is summarized in Fig. 1. This retrospective study was approved by the Institutional Review Board of the Second Affiliated Hospital, Zhejiang University School of Medicine (Zhejiang, China). The signed informed consent forms were waived. This study was conducted according to the Declaration of Helsinki. A total of 101 consecutive of patients from our institution who underwent arthroscopic rotator cuff treatment by a senior surgeon from June 2016 to December 2018 were included in this study. All of them received MRI before surgery and six to twelve months after surgery. Another 101 patients who underwent shoulder MRI due to discomfort of shoulder with no abnormality during the same period were randomly selected. The inclusion criteria for patients in this study included: (a) patients who underwent arthroscopic rotator cuff repair due to rotator cuff injury; (b) patients who had shoulder discomfort without significant abnormality in MR images; (c) patients operated by an experienced surgeon who had been performing shoulder arthroscopy for ten years; (d) patients undergoing surgery who received MRI for six to twelve months after operation. The exclusion criteria were as follows: (a) patients with other shoulder diseases; (b) Patients who had not undergone MRI in our institution within the allotted time.

2.2. Image acquisition

The MR images were performed based on two MR scanners including a 1.5 T scanners (SIEMENS MAGNETOM Aera 1.), and a 1.5 T MR scanner (MAGNETOM Avanto). Oblique coronal T2-weighted fat suppression of shoulder MRI was used in this study.

2.3. VOI segmentation and radiomics feature extraction

The VOI of MR images was interpreted independently by a musculoskeletal radiologist who had worked five years. The status of Re-RCT was evaluated by Sugaya typing in Fig. S1. Coronal T2 with fat
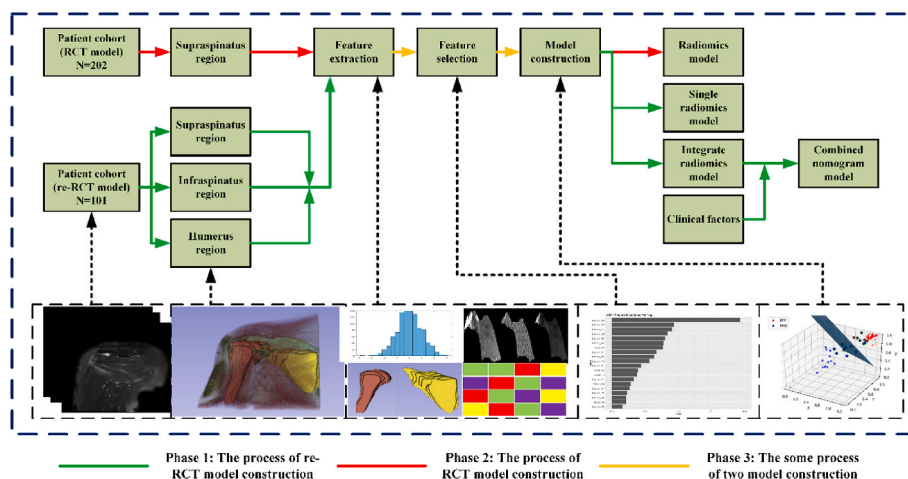

Fig. 1. The work flow of this study.

suppression was chosen for further assessment. The 3D VOI of supraspinatus in the oblique coronal position were independently and manually depicted by clinical radiologist using the ITK-SNAP software.[23] The VOI of humerus and infraspinatus were also depicted for 101 patients with RCT for further improving the prognosis performance of the Re-RCT prediction model. These VOI regions were evaluated by another experienced radiologist independently to confirm the stability of VOI. To estimate the different results from various MRI machines, the pre-processing of the image was applied before the feature extraction process.

After the delineation, we re-sampled the VOI pixels on the MATLAB 2018b software. All pixels of images were re-sampled to the size of $1 \times 1 \times 1$ mm^3 voxel size and the gray level in all images were normalized to a scale of 1–64. A total number of 547 features including intensity features, texture features, wavelet features and shape features were extracted based on MATLAB.

2.4. Radiomics feature selection

To decrease the errors of feature values due to different value scales, a normalization approach was utilized in this study before feature selection. A two-step feature selection method was applied to picking up the optimal radiomics features which had the best capacity for model construction. Firstly, the Wilcoxon-test method was used to select the significant features that distinguished between patients with RCT or Re-RCT. Only the features with *p-value*<0.05 were retained. Secondly, the maximum relevance minimum redundancy (MRMR)[24] algorithm was applied to assess the relevance and redundancy of each feature. The maximum relevance aimed to select the feature that has the highest correlation with the muscle status. The choice of minimum redundancy ensured that the selected features had minimum redundancy.

2.5. Radiomics signature building and feature analysis

To explore the prediction performance of radiomics features in RCT diagnosis and treatment, two models were constructed, based on RCT signature and postoperative Re-RCT signature, respectively.

For the development of pre-operative RCT signature, two individually independent datasets were used to develop optimal classifiers for different status of pre-operative RCT. These datasets were separated according to diagnostic time. The training dataset involved 70 patients with RCT and 70 patients without RCT. The validation dataset contained 30 patients with RCT and without RCT, respectively. A multiple regression logistic (MLR)[25] method was used to develop the pre-operative RCT model.

To predict the postoperative Re-RCT status, we developed a prognostic signature among 101 patients with RCT to predict the postoperative status of patients. Radiomics features extracted from three regions including supraspinatus, infraspinatus and humerus were used to improve the performance of this signature. Patients with RCT included 26 patients with Re-RCT and 75 patients without Re-RCT after surgery. Since statistics bias might occur due to imbalance in the dataset, we used a data balance method including oversampling, downsampling[26] and data generation, which was conducted by deleting or adding data randomly and reasonably. Firstly, 10 patients with Re-RCT and 10 patients without Re-RCT from the origin dataset were randomly organized as an independent validation cohort. Then, the retained patients were subjected to oversampling or undersampling by balance algorithm as a training cohort. A total of 65 patients without Re-RCT were undersampled to the amount of 50, and 16 patients with Re-RCT were oversampled to the amount of 50. Finally, a total of 100 people was used to develop the classifier. Ten-fold random experiments were employed to verify the stability of the results. The performance of this model developed by single type features and integrated features were also explored.

To obtain the signature with the best performance, we explored the

other two machine learning algorithms to construct the Re-RCT model involving the support vector machine (SVM)[27] and random forest (RF).[28] To consider the potential effectiveness of clinical characteristics for each patient, we built a clinical model and a nomogram model which combined the radiomics score and clinical factors. The backward search method with Akaike Information Criterion (AIC) were used to select the optimal clinical features in each test. The model with the lowest AIC value were selected as a model to classify patients with Re-RCT and without Re-RCT. The clinical features in each model were also recorded.

2.6. Radiomics model evaluation and feature analysis

For the pre-operative RCT prediction model, the performance of the prediction model was evaluated using area under the receiver operating characteristic curve (AUC). The AUC values were also reported with a 95% confidence interval (CI). The calibration of the prediction models was detected by using calibration curves accompanied by the Hosmer-Lemeshow (H-L) test. The calibration curves measured the consistency between the RCT probability and the actual RCT probability.[29] To explore the prediction performance of single features, univariate analysis was conducted and the nomogram was used to visualized the weight of selected features in the signature.

For the post-operative model evaluation, the mean value and variance of the AUC from the 10 experiments were calculated. We recorded the number and frequency of features used in each experiment. The higher the frequency of the appeared feature, the higher the importance of that feature in model construction.

2.7. Statistical analysis

All statistical tests used in this study were executed on MedCalc Statistical Software V15.2.2 or R software V3.4.1. Univariate analysis for clinical features was implemented by using the Chi-squared test or Mann-Whitney *U* test, as appropriate. A *p-value* < 0.05 in two-tailed analyses was considered to be statistically significant.

3. Results

3.1. Patient population

A patient dataset of 202 patients was used in this study, which included 101 patients with the status of normal rotator cuff tissue and another 101 patients with RCT. In the RCT dataset, 26 patients were diagnosed as Re-RCT after surgery. Non-significant clinical parameters were observed between the training cohort and validation cohort in the pre-operative data set, which ensured the uniformity of data distribution. The demographic characteristics of the subgroups classified by status of tear are summarized in Table 1. We evaluated whether there were statistically significant differences in the clinical parameters between the Re-RCT and recovery cohort by preoperative MRI (Table 2). Goutallier classification showed significant differences between patients with Re-RCT and recovery, while other clinical parameters showed non-significant differences between the two cohorts.

Table 1
The clinical characteristics of all patients.

Demographic or clinicopathologic characteristic	Training dataset (n = 140)	Validation dataset (n = 62)	p-value
Age			0.629
Range	19–78	18–79	
Mean ± Std	53.6 ± 12.6	52.6 ± 11.0	
Gender			0.589
Male	62	30	
Female	78	32	

Table 2
The clinical characteristics of RCT patients in preoperative MRI.

Demographic or clinicopathologic characteristic	Re-RCT dataset (n = 26)	Recovery dataset (n = 75)	p-value
Age			0.773
Range	49–78	43–79	
Mean ± Std	61.8 ± 7.7	61.3 ± 7.6	
Gender			0.899
Male	9	27	
Female	17	48	
Retraction distance (mm)			0.379
Range	5–42.6	8.3–47.5	
Mean ± Std	21.3 ± 9.1	19.5 ± 9.3	
Anteroposterior tear length (mm)			0.376
Range	2.2–30.6	3.1–35	
Mean ± Std	10.5 ± 9.1	19.5 ± 9.3	
Goutallier			**<0.0001**
Grade 1	10	3	
Grade 2	7	32	
Grade 3	3	36	
Grade 4	6	1	
Patte			0.1660
Grade 1	13	49	
Grade 2	7	19	
Grade 3	6	7	

3.2. Feature selection and feature evaluation

To construct the classifier for RCT, a total of 410 radiomics features with statistically significant differences between the two groups were retained after univariate analysis. The MRMR algorithm was used to decrease the redundancy of the feature set and build the optimal subset of complementary predictive features. Four highest MRMR-ranked features were selected to construct the preoperative RCT signature. Univariate analysis indicated that the *GLV_LLL* feature showed the best performance with an AUC of 0.954 (95%CI, 0.929–0.980). Nomogram for radiomics features showed that the *GLV_LLL* feature occupied the highest weight. The univariate analysis and nomogram are shown in Fig. 2A and B.

As for the classifiers of prognosis, Fig. 2C showed the number of features from the three regions involved in each experiment. Features extracted from the infraspinatus indicated the best performance in

discriminating the status of Re-RCT. As Fig. 2D showed, we also calculated the frequency of each radiomics features in all ten-fold experiments. The feature of *SZE_HHH* from the infraspinatus region had the most important weightage in predicting patients of Re-RCT. Wavelet-based features made the greatest contribution for model construction among all type of features.

3.3. Performance of the RCT radiomics model

When the proposed model was utilized in diagnosing the preoperative status of RCT, promising performances were observed in both the training and validation cohorts. The signature produced an AUC of 0.989 (95%CI:0.954–0.999) in the training cohort and 0.979 (95% CI:0.906–0.999) in the validation cohort by the MLR algorithm. The ROC curves of radiomics signature derived from the two data sets are shown in Fig. 3A and B.

By H-L testing, the training and validation signatures showed non-statistical significance with *p-value* = 0.9999 and *p-value* = 0.9626, respectively. The calibration curve is shown in Fig. S2. The equation of the radiomics model is as follows:

$$Radioscore = 1.5 + 0.0914 \times GLV\_LLL + 0.0746 \times inf\,2\,h\_LHH - 0.144$$
$$\times\ corrp - 0.1864 \times Skewness.$$

3.4. Performance of the prognosis-RCT radiomics model

For the prognosis Re-RCT radiomics prediction model, the signature obtained from the humerus region features displayed an average AUC of 0.662 ± 0.054 for the training cohort and 0.600 ± 0.064 for the validation cohort via ten-fold experiments. For the model developed by features derived from the supraspinatus region, better predictive performance was observed than the model based on the humerus region features, with an AUC of 0.812 ± 0.050 for the training dataset and 0.673 ± 0.089 for the validation dataset. The model generated by the infraspinatus region features also yielded satisfactory results in discriminating patient prognostic outcomes. The training data set yielded an average AUC of 0.879 ± 0.041, and an average AUC of 0.739 ± 0.069 for the validation dataset. The radiomics model based on multiple regions of interest, yielded the best performance amongst all models (training data set: 0.923 ± 0.017; validation data set: 0.790 ± 0.082). Based on the Student's t-test, the integrated model showed statistically
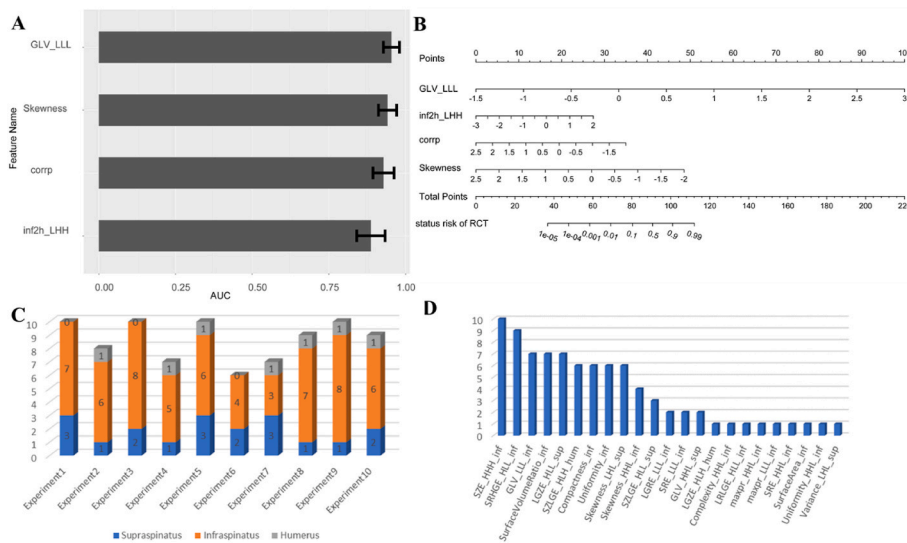

Fig. 2. The figure of radiomics feature analysis. (A): AUC and the 95% confidence interval (CI) values of radiomics features which develop the RCT model; (B) the radiomics nomogram for the RCT model; (C) the number of features from different regions in Re-RCT model by 10-fold test; (D) the frequency of features used in Re-RCT model by 10-fold test.
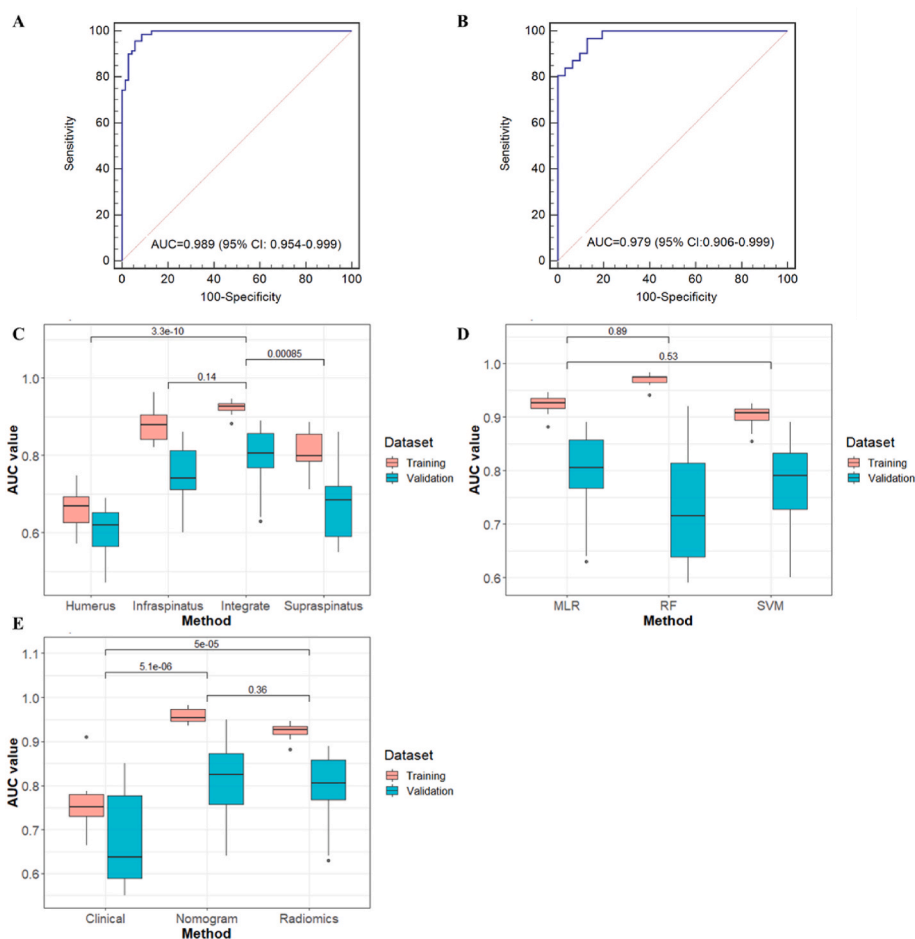
Fig. 3. The ROC curves of the rotator cuff features-based RCT classifier in the training dataset (A) and validation dataset (B). The boxplot of AUC between different Re-RCT predictive model. (C): The boxplot of AUC between different Re-RCT predictive model based on various VOI; (D): The boxplot of AUC between different Re-RCT predictive model based on various machine learning algorithm; (E): The boxplot of AUC between radiomics model, combined nomogram model and clinical model.

significant improvement from the humerus model (*p-value*<0.001) and supraspinatus model (*p-value*<0.001), while non-significant differences were observed in the infraspinatus model (*p-value* = 0.12). The boxplot of ten-fold experiments AUC value in the three models were plotted in Fig. 3C and the detailed AUC values of each experiment are summarized in Table S1 and Table S2.

The model developed by other machine learning algorithms also showed favorable results both in the training (SVM:0.901 ± 0.022; RF: 0.969 ± 0.011) and validation cohorts (SVM:0.776 ± 0.081; RF: 0.734 ± 0.109). While, comparing the validation, the performance of models based on the MLR method yielded better results than other methods. The performances of the various models based on different machine learning algorithms are depicted in Fig. 3D. The model based on clinical factors yielded significantly (*p-value*<0.0001) lower performance (training dataset: 0.758 ± 0.063 l validation dataset: 0.675 ± 0.108) than the radiomics model. The clinical factors used in each experiment are shown in Fig. S2. The combined nomogram model showed a better performance in predicting the status of Re-RCT (training dataset: 0.958 ± 0.015; validation dataset: 0.812 ± 0.088) than the radiomics model, via integrating both the radiomics score and clinical characteristics. However, there was non-significant improvement of the nomogram model versus radiomics model (*p-value* = 0.37). The AUC values of ten-fold experiments for the above models are presented in the boxplot in Fig. 3E. The detailed AUC values for each experiment are presented in Table S3.

4. Discussion

In this study, we investigated the utility of our radiomics model in the diagnosis of RCT and pre-operative prediction of Re-RCT, which was a grand new application of radiomics in rotator cuff injuries. A four-feature-based radiomics signature was observed to be effective for diagnosis of RCT, and thus, demonstrated the capabilities in distinguishing rotator cuff in MRI. This model could classify patients into RCT and non-RCT with an AUC of 0.979 in validation cohort studies, which is comparable to the reported performance of experienced radiologists.[30] For the prediction model of post-operative re-tear, by ten-fold independent experiments, the signature based on three different regions of interest achieved a promising performance. Furthermore, upon combining with clinical factors, the nomogram model in validation achieved a better functioning.

Radiomics methodologies have been widely applied in the diagnosis and prognosis of musculoskeletal tumors. Ritz et al. performed manual interpretation and textural analyses on MRI images of 116 cases of cartilage tumors to evaluate benign and malignant cartilage tumors.[21] Wu et al. combined CT image radiographic features and clinical parameters to develop a nomogram for predicting the survival of patients with high-grade osteosarcoma, which was superior to the clinical model.[22] The favorable predictive performance of two models based on radiomics features thus demonstrated the applicability of radiomics methodology in sports medicine and musculoskeletal diseases.

Clinicians often empirically evaluate rotator cuff injury by Fatty

infiltration, size of tear and other parameters from MRI when evaluating the repairability of the injury.[31–33] Occasionally, surgeons need to confirm the elasticity and quality of the tendon by pulling the torn tendon with a grasper during surgical operations, before deciding the method of repair.[34] In our study, the proposed radiomics model with promising performance could significantly improve the accuracy and speed in distinguishing torn tendon from healthy tendon. The accurate pre-operative prediction of Re-RCT prognosis is likely to lead to a better organized and more appropriate operation plan. For example, performing superior capsular reconstruction, or the transfer of latissimus dorsi muscle should be considered for patients with predicted poor prognosis from the model, to reduce the occurrence of re-tears and risks of a second operation.[35,36]

In the optimization process of MRMR methodology for radiomics feature selection, wavelet-based features had the highest importance in the two prediction models, suggesting the vital role of wavelet-based features in the domain of RCT diagnosis and Re-RCT prediction. The consistent results have been proven in previous studies on radiomics model construction.[37] The wavelet transformation splits imaging data into different frequency components on the three axes of the rotator cuff region, which may further explain the spatial heterogeneity at multiple scales within rotator cuff tissue. The *GLV_LLL* feature showed the best performance in classifying the status of RCT, which would have the best capacity to analyze the 3D structure of the tear region.

As for the Re-RCT model, we explored the prediction performance of radiomics features from three different rotator cuff regions. We observed that features from the infraspinatus yielded the best performance in predicting the prognosis status, which indicates that the status of prognosis were strongly correlated with the infraspinatus. This result was consistent with the study of Kim et al., which demonstrated that fatty infiltration of the infraspinatus, rather than of the supraspinatus or the subscapularis, led to poor muscle quality, which indicates poor prognosis.[38] By combing the features extracted from the infraspinatus and supraspinatus, the model showed better prediction performance which would further explain the correlation of prognosis status with rotator cuff spatial arrangement. To further improve the predictive capacity, some clinical parameters were also incorporated into the model. In the statistical analysis of clinical features, anteroposterior tear length and Goutallier classification factors were frequently used to construct the clinical model. This result confirmed the importance of anteroposterior tear length and Goutallier classification factors in predicting Re-RCT, despite the relatively poor performance of our clinical model compared to previous research.[15,39] Furthermore, the method of integrating other clinical parameters provided a feasible way to improve the performance of the radiomics model. The combined nomogram with a favorable performance provided us a brand-new and efficient diagnostic methodology for predicting prognostic status of Re-RCT.

Nevertheless, our study still had some limitations. Firstly, all patients with rotator cuff injury included in this study had surgical indications, which made it easier to distinguish the patient with RCT or not. Secondly, patients with RCT underwent ARCR from one experienced doctor, and data from only two MRI machines were included in the study, which lacked external verification. Although we conducted a data-balance method to correct for the data distribution, the relatively low number of only 26 patients with Re-RCT could also bring about some prediction error. In the future, we would verify the proposed model at multiple-centers with sufficient sample sizes.

5. Conclusion

This study developed and validated two models to classify the diagnosis of RCT and pre-operative prediction of Re-RCT. The radiomics model developed by four radiomics markers from the infraspinatus yielded a favorable performance in classifying RCT. The combined Re-RCT prognosis model developed using radiomics score and clinical parameters yielded better prediction accuracy than the clinical model and

radiomics alone. These newly-developed models could play a vital role in RCT diagnosis and Re-RCT prediction, which would guide clinicians in making individualized surgical decisions in the future.

Funding

Appendix A. Supplementary data

Supplementary data to this article can be found online at https://doi.org/10.1016/j.asmart.2024.03.003.

References

1. Tempelhof S, Rupp S, Seil R. Age-related prevalence of rotator cuff tears in asymptomatic shoulders. *J Shoulder Elbow Surg*. 1999;8(4):296–299.
2. Henry P, Wasserstein D, Park S, et al. Arthroscopic repair for Chronic massive rotator cuff tears: a systematic review. *Arthroscopy*. 2015;31(12):2472–2480.
3. Williams Jr G, Kraeutler MJ, Zmistowski B, Fenlin Jr JM. No difference in postoperative pain after arthroscopic versus open rotator cuff repair. *Clin Orthop Relat Res*. 2014;472(9):2759–2765.
4. Felsch Q, Mai V, Durchholz H, et al. Complications within 6 Months after arthroscopic rotator cuff repair: registry-based evaluation according to a core event set and severity grading. *Arthroscopy*. 2021;37(1):50–58.
5. Desai VS, Southam BR, Grawe B. Complications following arthroscopic rotator cuff repair and reconstruction. *JBJS Rev*. 2018;6(1), e5.
6. Miller BS, Downie BK, Kohen RB, et al. When do rotator cuff repairs fail? Serial ultrasound examination after arthroscopic repair of large and massive rotator cuff tears. *Am J Sports Med*. 2011;39(10):2064–2070.
7. Yang L, Zhang J, Ruan D, Zhao K, Chen X, Shen W. Clinical and structural outcomes after rotator cuff repair in patients with diabetes: a meta-analysis. *Orthop J Sports Med*. 2020;8(9), 2325967120948499.
8. Yang Y, Qu J. The effects of hyperlipidemia on rotator cuff diseases: a systematic review. *J Orthop Surg Res*. 2018;13(1):204.
9. Naimark M, Robbins CB, Gagnier JJ, et al. Impact of smoking on patient outcomes after arthroscopic rotator cuff repair. *BMJ Open Sport Exerc Med*. 2018;4(1), e000416.
10. Warrender WJ, Brown OL, Abboud JA. Outcomes of arthroscopic rotator cuff repairs in obese patients. *J Shoulder Elbow Surg*. 2011;20(6):961–967.
11. Harada GK, Arshi A, Fretes N, et al. Preoperative vitamin D deficiency is associated with higher postoperative complications in arthroscopic rotator cuff repair. *J Am Acad Orthop Surg Glob Res Rev*. 2019;3(7), e075.
12. Elkins AR, Lam PH, Murrell G. Duration of surgery and learning curve affect rotator cuff repair retear rates: a post hoc analysis of 1600 cases. *Orthop J Sports Med*. 2020; 8(10), 2325967120954341.
13. McColl AH, Lam PH, Murrell G. Are we getting any better? A study on repair integrity in 1600 consecutive arthroscopic rotator cuff repairs. *JSES Open Access*. 2019;3(1):12–20.
14. Xie Y, Liu S, Qu J, Wu P, Tao H, Chen S. Quantitative magnetic resonance imaging UTE-T2* mapping of tendon healing after arthroscopic rotator cuff repair: a longitudinal study. *Am J Sports Med*. 2020;48(11):2677–2685.
15. Kim JY, Park JS, Rhee YG. Can preoperative magnetic resonance imaging predict the reparability of massive rotator cuff tears? *Am J Sports Med*. 2017;45(7):1654–1663.
16. Bierry G, Palmer WE. Patterns of tendon retraction in full-thickness rotator cuff tear: comparison of delaminated and nondelaminated tendons. *Skeletal Radiol*. 2019;48 (1):109–117.
17. Mário L, Rachelle B, Yemisi T, Johnston Renea V, Ca HN, Flávio F. Magnetic resonance imaging, magnetic resonance arthrography and ultrasonography for assessing rotator cuff tears in people with shoulder pain for whom surgery is being considered. *Cochrane Database Syst Rev*. 2013;(9).
18. Yoshida M, Collin P, Josseaume T, et al. Post-operative rotator cuff integrity, based on Sugaya's classification, can reflect abduction muscle strength of the shoulder. *Knee Surg Sports Traumatol Arthrosc*. 2018;26(1):161–168.
19. Sugaya H, Maeda K, Matsuki K, Moriishi J. Repair integrity and functional outcome after arthroscopic double-row rotator cuff repair. A prospective outcome study. *J Bone Joint Surg Am*. 2007;89(5):953–960.
20. Juhan T, Stone M, Jalali O, et al. Irreparable rotator cuff tears: current treatment options. *Orthop Rev*. 2019;11(3):8146.
21. Fritz B, Müller DA, Sutter R, et al. Magnetic resonance imaging-based grading of cartilaginous bone tumors: added value of quantitative texture analysis. *Invest Radiol*. 2018;53(11):663–672.
22. Wu Y, Xu L, Yang P, et al. Survival prediction in high-grade osteosarcoma using radiomics of diagnostic computed tomography. *EBioMedicine*. 2018;34:27–34.
23. Yushkevich PA, Piven J, Hazlett HC, et al. User-guided 3D active contour segmentation of anatomical structures: significantly improved efficiency and reliability. *Neuroimage*. 2006;31(3):1116–1128.
24. Unler A, Murat A, Chinnam RB. Mr 2 PSO : a maximum relevance minimum redundancy feature selection method based on swarm intelligence for support vector machine classification. *Inf Sci*. 2010;181(20).

25. Yu SC, Qi X, Hu YH, Zheng WJ, Wang QQ, Yao HY. [Overview of multivariate regression model analysis and application]. Chinese *Zhonghua Yufang Yixue Zazhi*. 2019 Mar 6;53(3):334–336. https://doi.org/10.3760/cma.j.issn.0253-9624.2019.03.020. PMID: 30841679.
26. Nanni L, Fantozzi C, Lazzarini N. Coupling different methods for overcoming the class imbalance problem. *Neurocomputing*. 2015;158.
27. Chang Chih-Chung, Lin Chih-Jen. LIBSVM: a library for support vector machines. *ACM Trans. Intell. Syst. Technol.* 2011;27.
28. Breiman L. Random forests. *Mach Learn*. 2001;45(1):5.
29. Kramer AA, Zimmerman JE. Assessing the calibration of mortality benchmarks in critical care: the Hosmer-Lemeshow test revisited. *Crit Care Med*. 2007;35(9): 2052–2056.
30. Huang T, Liu J, Ma Y, Zhou D, Chen L, Liu F. Diagnostic accuracy of MRA and MRI for the bursal-sided partial-thickness rotator cuff tears: a meta-analysis. *J Orthop Surg Res*. 2019;14(1):436.
31. Liem D, Lichtenberg S, Magosch P, Habermeyer P. Magnetic resonance imaging of arthroscopic supraspinatus tendon repair. *J Bone Joint Surg Am*. 2007;89(8): 1770–1776.
32. Shin YK, Ryu KN, Park JS, Jin W, Park SY, Yoon YC. Predictive factors of retear in patients with repaired rotator cuff tear on shoulder MRI. *AJR Am J Roentgenol*. 2018; 210(1):134–141.

33. Lee S, Park I, Lee HA, Shin SJ. Factors related to symptomatic failed rotator cuff repair leading to revision surgeries after primary arthroscopic surgery. *Arthroscopy*. 2020;36(8):2080–2088.
34. Lee YS, Jeong JY, Park CD, Kang SG, Yoo JC. Evaluation of the risk factors for a rotator cuff retear after repair surgery. *Am J Sports Med*. 2017;45(8):1755–1761.
35. Adams CR, DeMartino AM, Rego G, Denard PJ, Burkhart SS. The rotator cuff and the superior capsule: why we need both. *Arthroscopy*. 2016;32(12):2628–2637.
36. Lee KT, Mun GH. A systematic review of functional donor-site morbidity after latissimus dorsi muscle transfer. *Plast Reconstr Surg*. 2014;134(2):303–314.
37. Xu L, Yang P, Liang W, et al. A radiomics approach based on support vector machine using MR images for preoperative lymph node status evaluation in intrahepatic cholangiocarcinoma. *Theranostics*. 2019;9(18):5374–5385.
38. Kim JR, Cho YS, Ryu KJ, Kim JH. Clinical and radiographic outcomes after arthroscopic repair of massive rotator cuff tears using a suture bridge technique: assessment of repair integrity on magnetic resonance imaging. *Am J Sports Med*. 2012;40(4):786–793.
39. Duong J, Lam PH, Murrell G. Anteroposterior tear size, age, hospital and case number are important predictors in repair integrity: an analysis in 1962 consecutive arthroscopic single row rotator cuff repairs. *J Shoulder Elbow Surg*. 2020;30(8): 1907–1914.